

Assessment and Modeling of the Vulnerability of Regional Aquifers to Anthropogenic Perturbations

Abdul Ghafoor^{1*}, Hayfa Habes Almutairi², Munthir Almoslem³, Saifullah^{3,4},
Khalid Turk¹, Muhammad Munir⁵, Faisal Zeineldin¹, Shafaqat Ali^{6,7}

¹ Water and Environmental Study Centre, King Faisal University Al-Ahsa, Saudi Arabia

² Department of Chemistry, College of Science, King Faisal University, Al-Ahsa, 31982, Saudi Arabia

³ Department of Environmental Health, College of Public Health, Imam Abdulrahman Bin Faisal University, Dammam, Saudi Arabia

⁴ Institute of Soil and Environmental Sciences, University of Agriculture, Faisalabad, Pakistan

⁵ Date Palm Research Center of Excellence, King Faisal University, Al-Ahsa 31982, Saudi Arabia

⁶ Department of Environmental Sciences, G.C. University Faisalabad, Faisalabad, Pakistan

⁷ Department of Biological Sciences and Technology, China Medical University, Taichung 40402, Taiwan

* Corresponding author's e-mail: abdul822@gmail.com

ABSTRACT

Water is at the core for achieving all 17 sustainable development goals (SDGs). The current study was performed for the appraisal and modeling of the vulnerability of regional aquifers to anthropogenic perturbations. Samples of water were examined to determine their physical and chemical properties. pH of groundwater varied from a value of 7.08 to a value of 8.46. Total dissolved solids (TDS) varied from 1048–1580 mg·L⁻¹. Results revealed that 79% of Ca²⁺, 47.3 % of Mg²⁺, and 100% of Na⁺ and Cl⁻ in water samples exceeded the standard permissible limits. The aquifer vulnerability index (AVI) revealed that Neogene aquifer was categorized as high vulnerability to extremely high vulnerability class of risk of contamination. AVI index method was also performed for the other major aquifers demonstrating that Dammam aquifer was categorized in the high vulnerability class, whereas Er Radhuma and Aruma categorized as moderately vulnerable to contamination. This study demonstrated an integrated model to help investigate the vulnerability of regional aquifers and highlighted the need for continuous monitoring campaigns to investigate the effects of anthropogenic activities on aquifers to make timely and effective decisions.

Keywords: groundwater, salinity, aquifer vulnerability index, water types, water quality.

INTRODUCTION

Water is at the core for achieving all 17 sustainable development goals (SDGs) (Fonseca et al., 2020). Water scarcity fueled by its contamination has become a major issue worldwide. Groundwater is an essential resource to meet the demands of humans for domestic, industrial, and irrigation use. In addition to salinity as one primary indicator of water quality, contamination of groundwater with pollutants is a matter of serious concern as intake of pollutants through drinking water may lead to chronic and acute health risks

(Al-Omran et al., 2016; Chen et al., 2019; Phan et al., 2023; El-Sayed and Elgendy, 2024). Continued use of poor-quality groundwater for agriculture and drinking purposes could pose a serious threat to the ecosystem, thus, warranting continuous assessment of such water resources.

Groundwater monitoring and quality assessment campaigns in the Arabian Peninsula have recently recognized that the region's groundwater resources are seriously degrading in quality as a result of ongoing urbanization, agricultural development, and heavy use of pesticides, fertilizers, and animal waste (Abdel-Satar et al.,

2017; Al-Omran et al., 2018; Iqbal et al., 2018). For sustainable utilization of groundwater, it is highly desirable to apply integrated approaches for groundwater resource management guided by continuous assessment of variation in groundwater hydro-geochemical process, and development of decision support tools to evaluate the future scenarios, thus, leading to more robust and sustainable solutions proactively (Ahmad and Al-Ghouti, 2020; El-Sayed et al., 2023). As a starting point, a better understanding of hydrochemical processes that govern the quality and composition of groundwater as a result of rock–water interactions, redox reactions, evaporation, and dilution due to precipitation is critically important. This will also help to get an insight into the spatiotemporal variation in groundwater chemistry influenced by these processes. Routinely, this can be accomplished using graphical analysis including Piper, Durov, Ternary, and Schoeller diagrams (Piper, 1944; Al-Omran et al., 2018; Alghamdi et al., 2020). However, modeling the vulnerability of aquifers, as a tool for decision-making, planning, and law enforcement, can provide additional benefits for securing fresh and clean water, especially in rural areas, where the groundwater is more susceptible to pollution due to indiscriminate rural agricultural and domestic practices (Van Stempvoort et al., 1993).

Three fundamental approaches for groundwater vulnerability assessment have been adopted by scientists so far (Gogu and Dassargues, 2000; Yu et al., 2010). According to the index approaches, evaluation of individual hydrogeological parameters is based on a subjective rating (Van Stempvoort et al., 1993), whereas physically-based approaches rely on simulating physical processes that take place in any hydrogeological system under consideration (Kumar et al., 2015). The statistical approaches strive to predict the concentration levels of pollutants or the possibility of contamination taking place based on correlations between the characteristics of the aquifer, sources of the pollutants, and occurrence of the pollutants derived from monitoring (Masetti et al., 2009). Among more than fifty methods available for determining groundwater vulnerability, index-based techniques such DRASTIC (Aller et al., 1987; Dawood et al., 2022), SINTACS, EPIK, and aquifer vulnerability index (AVI) are becoming more popular since they can be applied in a range of scenarios and require comparatively less data (Kumar et al., 2015). The aquifer vulnerability

index, based on two factors: sediment layer thickness and the hydraulic conductivity for each layer, is a promising approach. Using hydrogeologic and/or soil data, this method assigns low to high groundwater contamination vulnerability ratings for different parts of the land. When identifying groundwater conservation areas or selecting potential sites for future land use, the AVI approach is very useful (Van Stempvoort et al., 1993; Raju et al., 2014). The Al-Ahsa region in Saudi Arabia's Eastern Province relies primarily on groundwater to meet its drinking water and irrigation needs. The groundwater in the region is stored in the Neogene, Dammam, Umm-Er-Radhuma, and Aruma aquifers. The primary concern is that these aquifers are vulnerable to pollution due to increased anthropogenic activities in recent decades. Given that, site-specific studies have clear advantages for groundwater management for that particular area, the primary goal of the current study is to investigate the hydrochemical characterization and modelling the aquifer vulnerability for better understanding the hydrogeological behavior of the aquifers under consideration and to identify areas in terms of susceptibility to pollution. Although the geological complexity of other aquifers would limit the transferability of the results, the approach would still assist planners and decision-makers in preventing aquifers from further contamination in other groundwater-dependent regions that have already been or will be the subject of intense anthropogenic activities in the foreseeable future.

MATERIALS AND METHODS

The study area

Al-Ahsa Oasis in Saudi Arabia's Eastern Province is situated 320 km southeast of the capital Riyadh. It is positioned between 25° 05' and 25° 40' northern latitude and 49° 10' and 49° 55' eastern longitudes (Fig. 1). The climate of the region is arid to semi-arid desert. Summers are blisteringly dry while winters are pleasant with sporadic showers. The air temperature varies from –2.6 to 52.3 °C, with an average annual precipitation of roughly 70.3 mm (Al-Zarah, 2007). Al-Ahsa, centered around the city of Al-Hofuf, is located approximately 70 km from the Gulf coast,

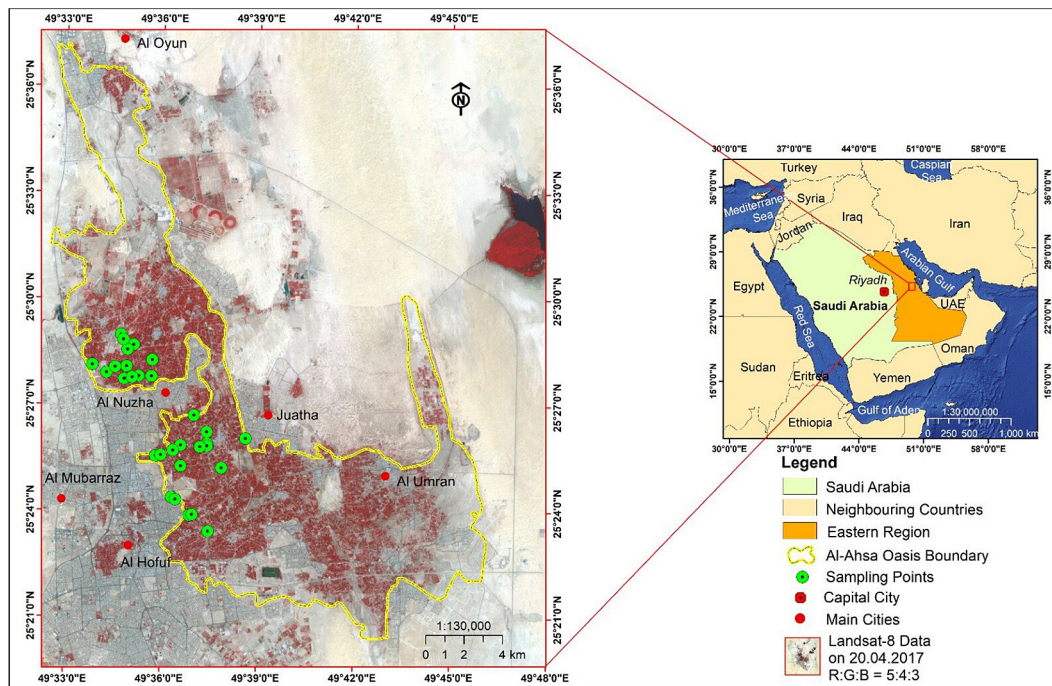


Figure 1. General layout and location of the study area showing monitoring sites

near the old port of Al-Uqayr, and has an altitude of 130 to 160 meters above sea level.

The hydrogeology

The sediments in the study area consists of carbonates, sulfates, and some marl and shale. With a slope that rises from the west to the east, the overall thickness varies between 800 and 2500 metres. The vast Euphrates-Gulf-Rub Al Khali Basin also includes the Al-Ahsa springs (Bakiewicz et al., 1982). Neogene, Umm-Er-Radhuma, Dammam, and Arum aquifers make up a complex multi-aquifer system. The water flow of Al-Ahsa Oasis originates from this aquifer system (Al Tokhais and Rausch, 2008). Intense fractures along the Ghawar anticline formed a preferential flow path. They connect different aquifers and allow groundwater to be released into the Al Ahsa Oasis. Hydrochemical data, isotope-hydrogeological data, temperature data and hydraulic information collectively show that the water flowing from the karst springs at Al Ahsa in the Neogene originated from the deeper Umm Er Radhum aquifer (Bakiewicz et al., 1982; Al Tokhais and Rausch, 2008).

Methodology

In order to evaluate the quality of the groundwater in the area, Al-Ahsa Irrigation and

Drainage Authority (HIDA) has launched an extensive groundwater sampling program. In the current study, samples from the nineteen wells dispersed throughout the study region were used to cover variation in the groundwater status. Wells were pumped for five to ten minutes before the collection of the samples to minimize the effects of static water. A composite representative sample from eight samples was collected from each sampling location. The geo-location of each well was determined with a Handheld GPS. Shanghai, China). After collection, samples were stored in a refrigerator at 4 °C before analysis for physicochemical properties, and the concentrations of Na^+ , K^+ , Ca^{2+} , Mg^{2+} , HCO_3^- , Cl^- , and SO_4^{2-} (APHA, 2005; Rice et al., 2012; Acharya et al., 2018). To plot Piper and Durov diagrams, WQChartPy package in Python (Yang et al., 2022) was used. The descriptive statistics, and the spatial distribution of the variables were obtained with R package gstat (Pebesma, 2004) in R statistical software (version 3.6.3).

The aquifer vulnerability index

The main reason for using this index was the information available for the study area, since the AVI takes into account two parameters. The first is each sedimentary layer's thickness (D) above the topmost aquifer, and

the second is each layer's hydraulic conductivity (K). Thus, the hydraulic resistance (C) for layers 1 to i can be calculated with:

$$C = \sum_{i=1}^i \frac{D_i}{K_i} \quad (1)$$

where: C is hydraulic resistance; D is the thickness of layer; and K is the hydraulic conductivity of layer.

RESULTS AND DISCUSSION

Hydrogeochemistry

Hydrogeochemical parameters are presented in Table 1. pH is a crucial parameter for determining whether water is acidic or alkaline in nature (Nasr and Zahran, 2014). The samples in the current study were slightly neutral to alkaline with pH ranged between 7.08 and 8.46. pH values from the current study were well within the range of 6.5 to 8.5 for drinking water guidelines (WHO, 2017). Electric current conducts poorly through pure water. Water's electrical conductivity (EC) increases as ion concentration rises. A higher EC indicates an elevated salt concentration and vice versa. The maximum EC in the current study was recorded as 2099 $\mu\text{S}/\text{cm}$, and the minimum was 1664 $\mu\text{S}/\text{cm}$. total dissolved solids (TDS) is a regularly used indication of the appropriateness of water for various applications. It is made up of a wide spectrum of salts and minerals, both organic and inorganic. TDS in drinking water has an optimal threshold of 500 $\text{mg}\cdot\text{L}^{-1}$, while the upper limit is 1000 $\text{mg}\cdot\text{L}^{-1}$ (WHO, 2017). Compared to WHO limits (WHO, 2017) of TDS in drinking water, all samples in the current study exceeded the WHO standard (1000 $\text{mg}\cdot\text{L}^{-1}$) with a range of 1048–1322 $\text{mg}\cdot\text{L}^{-1}$. According to our findings, which are consistent with those of other researchers who also noticed elevated TDS in well water samples from other parts of Saudi Arabia (Abdel-Satar et al., 2017), implying that evaporation and chemical weathering are the primary factors influencing the elevated TDS in groundwater of arid and semi-arid regions (Aly et al., 2015; Al-Omran et al., 2016). The regional distribution of TDS's increasing and decreasing trends are shown in Figure 2. The high TDS levels in the area could perhaps be attributed to the drawdown effect of the high pumping rate, which resulted in a blend of freshwater and salty water being

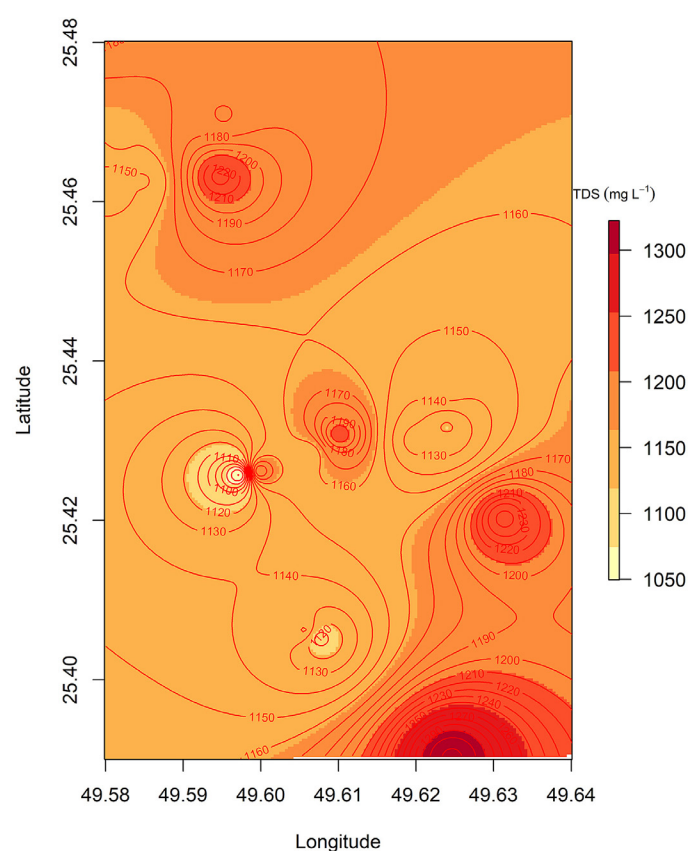
acquired from deeper aquifers, and thus, lowering the groundwater quality (Al-Zarah, 2007). The hydrogeochemical parameters derived from our analysis differ relatively from the historical data, and there are some noteworthy trends in the hydrogeochemical parameter values over time. For example, the Na^+ ion in the current study exhibited an increasing trend with concentrations ranging from 427.0 and 1545 $\text{mg}\cdot\text{L}^{-1}$ compared to 140–720.3 $\text{mg}\cdot\text{L}^{-1}$ determined by Al-Zarah (2007). Comparing the current study's Cl^- concentration to that of Al-Zarah (2007) 205–1155 $\text{mg}\cdot\text{L}^{-1}$, it exhibited a rather similar range (436–1068 $\text{mg}\cdot\text{L}^{-1}$). While Al-Zarah (2007) reported Ca^{2+} concentrations of 120–336 $\text{mg}\cdot\text{L}^{-1}$, the current study's Ca^{2+} concentration ranged from 160–425 $\text{mg}\cdot\text{L}^{-1}$. The concentration of Mg^{2+} in the current study was between 70–193 $\text{mg}\cdot\text{L}^{-1}$ compared to 45.81–131.1 $\text{mg}\cdot\text{L}^{-1}$ found by Al-Zarah (2007). The pH range showed a slightly increasing trend of 7.08 to 8.46 in the current study compared to a range of 6.8 to 7.3 reported by Al-Zarah (2007). A cursory analysis of the dataset indicates that Na^+ was the cation in significantly high concentrations, ranging from 427 to 1545 $\text{mg}\cdot\text{L}^{-1}$. Similarly, compared to anions Cl^- and HCO_3^- were quantitatively more abundant than anion SO_4^{2-} .

Given that saltwater intrusion from the coast mostly controls the amount of sodium (Na^+) in groundwater, the study area's high Na^+ values may be related to its closeness to the Gulf Coast. $\text{Cl}^- > \text{HCO}_3^- > \text{SO}_4^{2-}$ is the anion concentration order. Subsequent analysis showed that the levels of 79% of Ca^{2+} , 47.3% of Mg^{2+} , and 100% of Na^+ and Cl^- in water samples exceeded the threshold limits for drinking water (WHO, 2008, 2017). A correlation study between the main ions and the physicochemical parameters under investigation is shown in Figure 3. TDS and Cl^- have a positive association ($R = 0.49$, $p < 0.05$). Between the Na^+ , Mg^{2+} ($R = 0.94$, $p < 0.001$), and Ca^{2+} ($R = 0.92$, $p < 0.001$), there was a significant positive association found. The concentration of HCO_3^- was shown to have a strong positive connection with that of Na^+ , Ca^{2+} , and Mg^{2+} ions, suggesting that the minerals dolomite and calcite have dissolved. An affirmative association was seen between Cl^- and Mg^{2+} ($R = 0.44$, $p < 0.05$), suggesting that seawater intrusion has an impact on hydrogeochemistry (El-Sayed et al., 2023).

The mineralogy and geochemistry of the aquifer dictate the temporal and geographical variability of groundwater hydrogeochemical processes. The main ions in the solution phase

Table 1. Descriptive statistics of physicochemical parameters of water samples

Specification	Units	Min	Max	Median	Mean	Std. dev	CV
pH	–	7.08	8.46	7.46	7.52	0.36	0.05
EC	$\mu\text{S}/\text{cm}$	1664	2099	1830	1850	95.87	0.05
TDS	$\text{mg}\cdot\text{L}^{-1}$	1048	1322	1153	1165	60.47	0.05
Ca^{2+}	$\text{mg}\cdot\text{L}^{-1}$	160.0	425.0	274.0	288.8	86.10	0.30
Mg^{2+}	$\text{mg}\cdot\text{L}^{-1}$	70.00	193.0	148.00	136.8	40.27	0.29
Na^+	$\text{mg}\cdot\text{L}^{-1}$	427.0	1545	1072	999.5	367.1	0.37
K^+	$\text{mg}\cdot\text{L}^{-1}$	10.00	31.00	17.00	18.95	6.36	0.34
Cl^-	$\text{mg}\cdot\text{L}^{-1}$	436.0	1068	742.0	778.4	169.48	0.22
SO_4^{2-}	$\text{mg}\cdot\text{L}^{-1}$	61.00	99.00	88.00	85.08	10.61	0.12
HCO_3^-	$\text{mg}\cdot\text{L}^{-1}$	266.0	607.0	470.0	461.6	102.49	0.22

**Figure 2.** Contour map of TDS illustrating spatial variation in the groundwater of the study area

and their interactions with other clay minerals are greatly impacted by the mineral compositions of the aquifer (Chen et al., 2019). Figure 4 illustrates the relationships between selected water quality parameters to identify and understand the processes regulating groundwater hydrogeochemistry of the study area. The Na^+ vs. Ca^{2+} scatter plot (Figure 4a) indicated that cation exchange may be the cause of the groundwater's higher than average Na^+ levels. The preferential adsorption of Ca^{2+} and the concurrent release of Na^+ ions are caused

by the cation exchange mechanism in the aquifer's clay minerals. Another helpful indication to validate the process of ion exchange between groundwater and its mineralogical composition is the relationship between $(\text{Na}^+ - \text{Cl}^-)$ (meq/L) and $(\text{Ca}^{2+} + \text{Mg}^{2+} - \text{SO}_4^{2-} - \text{HCO}_3^-)$ (meq/L) (Figure 4c) (Ettazarini, 2005; Carol et al., 2012). The effects of minerals of silicate and carbonate were explored by $(\text{Ca}^{2+} + \text{Mg}^{2+})$ vs. $(\text{HCO}_3^- + \text{SO}_4^{2-})$ scatter diagram (Figure 4d). The ratio of this relationship was 3.3, and the correlation coefficient

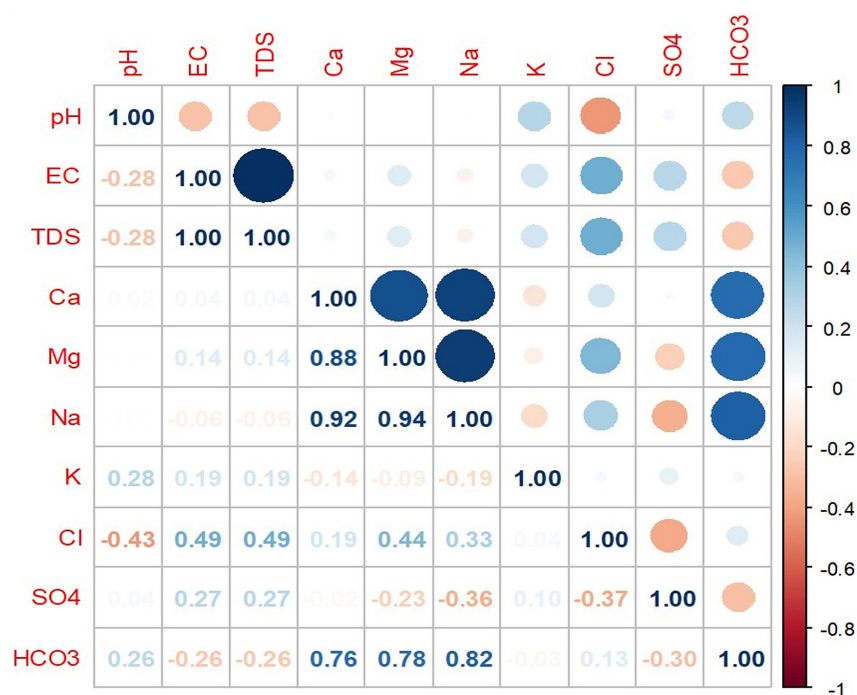


Figure 3. Correlation matrix of the physicochemical parameters

was 0.65, suggesting that minerals of carbonate are the main source of Ca^{2+} and Mg^{2+} in comparison to silicate minerals, which is also confirmed by the positive correlation between Ca^{2+} and HCO_3^- (Figure 4b). Other researchers have also noted the impact of carbonate mineral dissolution on aquifer hydrochemistry (Al-Omran et al., 2017; Saleh et al., 2023).

Water types

For geochemical grouping of groundwater, and to anticipate the nature and origin of water types, Python and WQChartPy (Yang et al., 2022) was used to produce Piper and Durov diagrams. The ionic composition of multiple water samples is shown using piper diagrams (Fig. 5), which also show trends between the samples (Piper, 1944). In the cation triangle, water samples are located in the sodium dominance while in the anion triangle, chloride predominance is clear. The Durov diagram (Fig. 6) also confirmed that most water samples had high salinity. The group of Na^+ - Ca^{2+} - Mg^{2+} - Cl^- made up 78.94% of the samples, followed by Na^+ - Mg^{2+} - Ca^{2+} - Cl^- (10.5%) and both Na^+ - Ca^{2+} - Mg^{2+} - HCO_3^- and Na^+ - Ca^{2+} - Cl^- (5.25%).

Although aquifers recorded many water types, but dominant water type in aquifers is Na-Cl type, indicating the effects of seawater intrusion on groundwater geochemistry (Aly et al., 2015).

In line with the discoveries of others (Al-Zarah, 2007) we have ascertained that Na^+ is the predominant cation, succeeded in decreasing order by Mg^{2+} , Ca^{2+} , and K^+ , whereas the pattern of anion concentration is $\text{Cl}^- > \text{SO}_4^{2-} > \text{HCO}_3^-$. In addition to region's lithology, which primarily consists of sandy, sandy limestone, marl and shale, subordinate sandstones and siltstones, and alluvial sediments primarily made up of CaCO_3 and limestone, the cation exchange sites selectively absorb Ca^{2+} and Mg^{2+} while releasing Na^+ in water, indicating a direct cationic exchange may be the underlying process (Al-Omran et al., 2018).

Modelling vulnerability of aquifers

The AVI index approach was performed. According to the AVI vulnerability index approach, groundwater vulnerability is categorized into five levels (very low, low, medium, high, and very high) (Van Stempvoort et al., 1993). Hydraulic conductivity (K) is a key characteristic in the AVI vulnerability technique that is associated with the aquifer's ability to transfer pollutants and water (Table 2). Higher values increase the aquifer's susceptibility to contamination and water moving more quickly from the source to groundwater (Aller et al., 1987). K – values can be derived from measurements or readily available soil databases, pedotransfer functions (Wösten et al., 2001), and soil surveys (Bouma

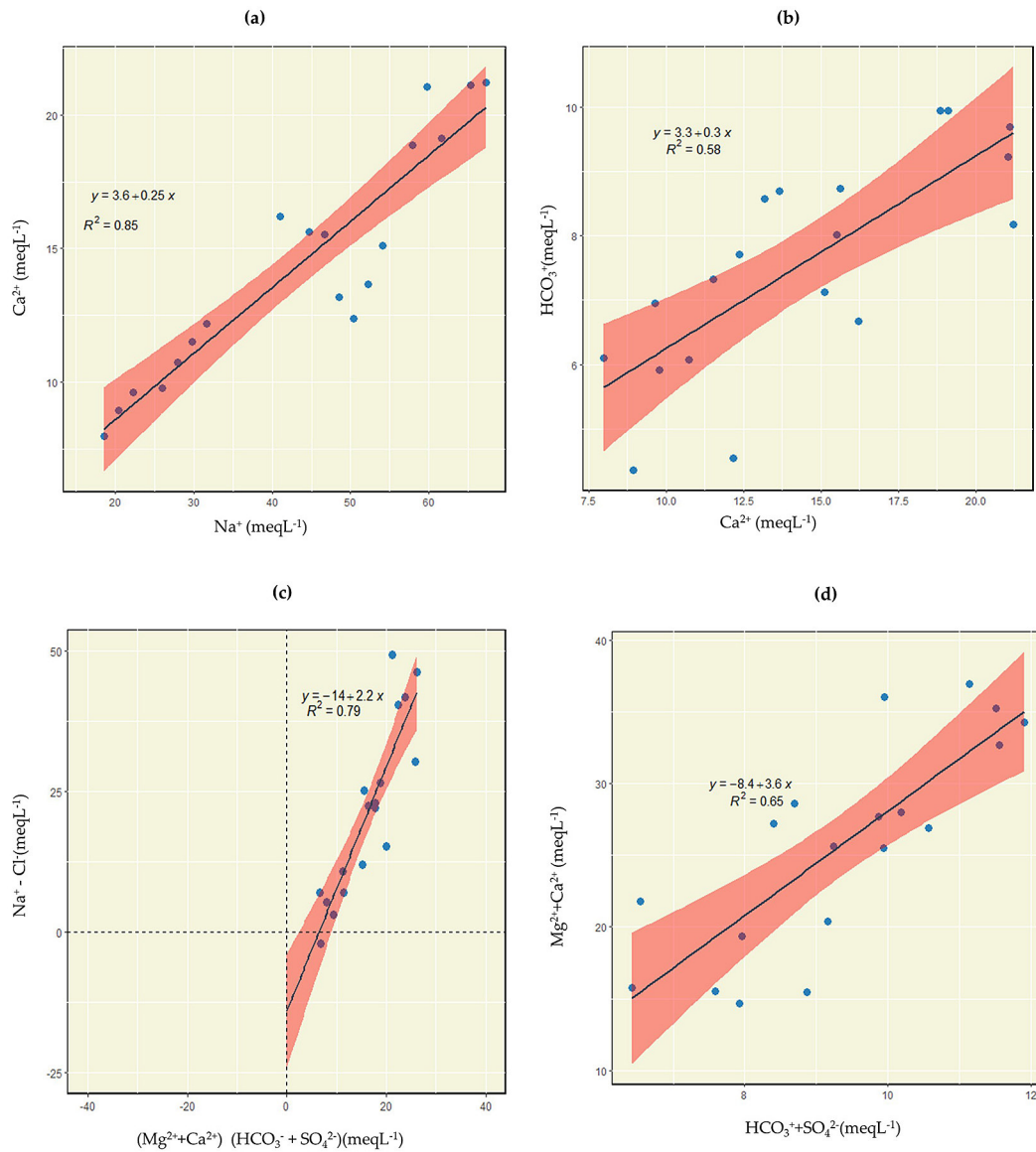


Figure 4. Illustration of effects of mineralogy and geochemistry on groundwater hydrogeochemical characterization (a) Na^+ vs. Ca^{2+} ; (b) Ca^{2+} vs. HCO_3^- ; (c) $(\text{Ca}^{2+} + \text{Mg}^{2+}) - (\text{HCO}_3^- + \text{SO}_4^{2-})$ vs. $\text{Na}^+ - \text{Cl}^-$; (d) $(\text{Ca}^{2+} + \text{Mg}^{2+})$ vs. $(\text{HCO}_3^- + (\text{SO}_4^{2-}))$

1989). Hydraulic conductivity (K) obtained from the easily accessible databases (Clapp and Hornberger, 1978) were well representative of the sediment units of the sandy and sandy loam vadose zone of the current study area. Utilizing the AVI approach, the hydraulic resistances of the Neogene aquifer range from 3.07 to 10.07 days. Neogene aquifer was classified as either extremely highly vulnerable or highly vulnerable, representing an area of 47.37% and 52.63%, respectively for extremely highly or highly vulnerable to contamination (Table 3). The AVI Index method was also performed for the other major aquifers (Dammam, Umm Er Radhuma, and Aruma) in Al-Ahsa (see Table 4 and Figure 7).

Hydraulic conductivity for these aquifer systems was obtained from Al-Tokhais and Rausch (2008). Figure 7 also shows the geology, hydrogeology, and flow of the aquifer systems (Mukhopadhyay et al., 1996; Al Tokhais and Rausch, 2008). The hydraulic resistances of Dammam, Umm Er Radhuma, and Aruma aquifers vary between 30 to 178 days. While the Dammam aquifer is categorized as highly vulnerable, Er Radhuma and Aruma exhibit moderate vulnerability to the risk of contamination. This is further illustrated in Figure 7, with red color being highly vulnerable and yellow-colored regions being moderately vulnerable regions. This emphasizes the fact that the thinner the layers above the aquifer will

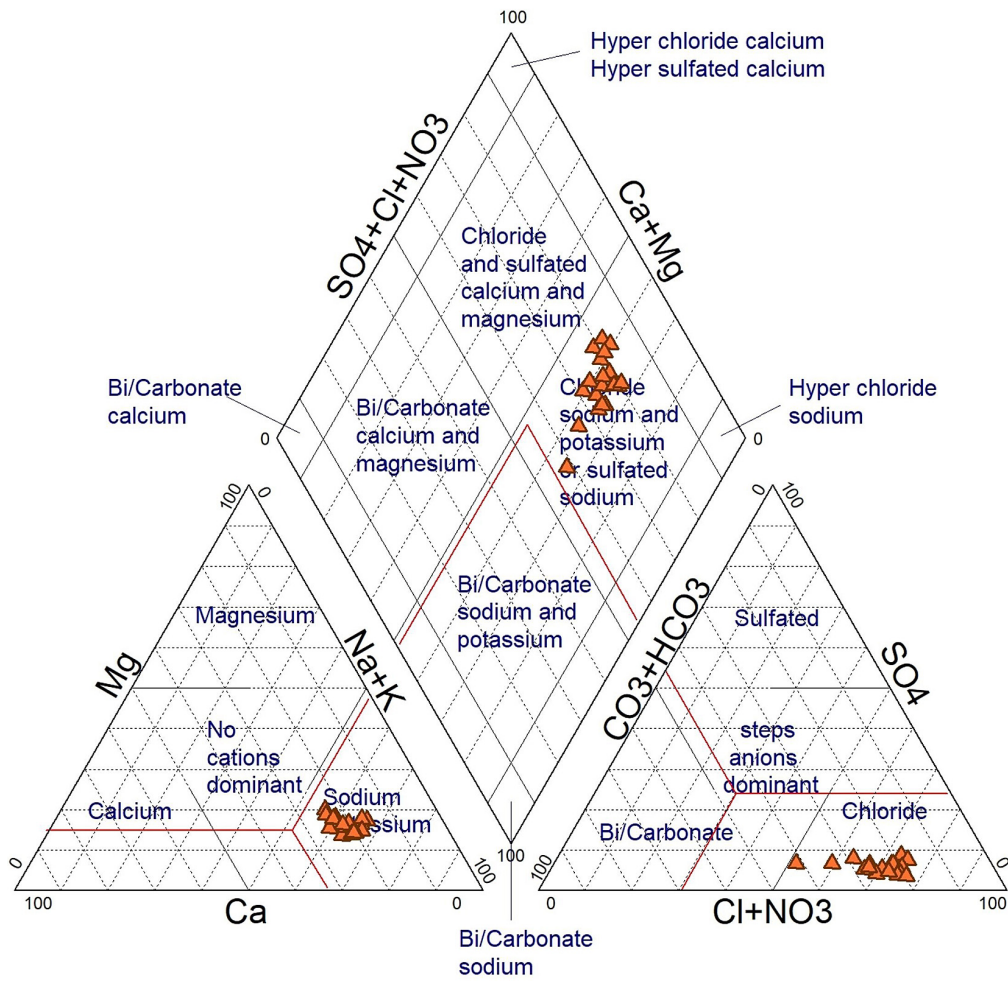


Figure 5. Piper diagram for groundwater samples of the study area

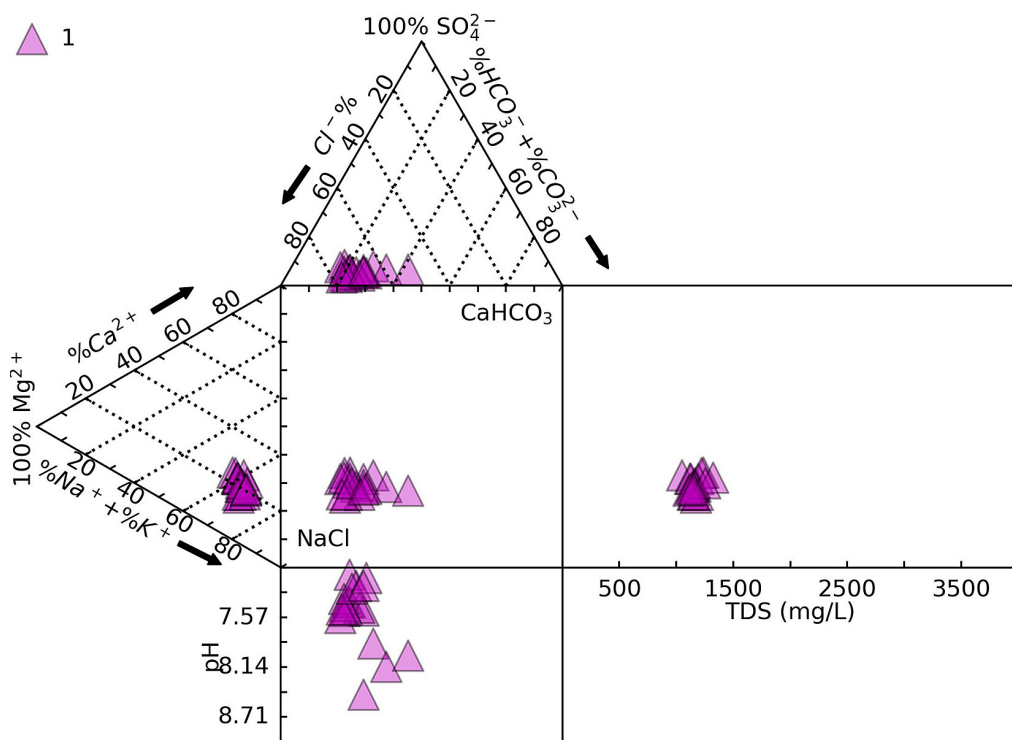


Figure 6. Durov diagram for groundwater samples of the study area

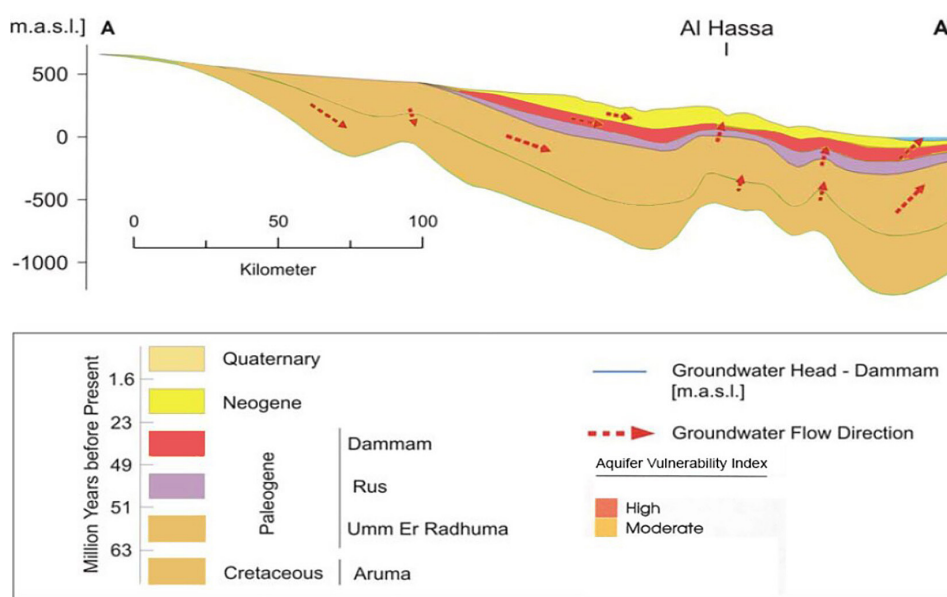


Figure 7. Illustration of hydrogeology, general groundwater flow direction, and the vulnerability classes of the aquifers. Unit for x-axis is elevation in meters above sea level (m.a.s.l)

Table 2. Relation between hydraulic resistance and aquifer vulnerability index classes

Hydraulic resistance (C) (Years)	Log (C)	Vulnerability (AVI)
0–10	< 1	Extremely high
10–100	1–2	High
100–1,000	2–3	Moderate
1000–10,000	3–4	Low
> 10,000	> 4	Extremely low

Table 3. AVI classes and hydraulic resistance for sampling locations of the study area

Sr No	Soil texture	K (m/d)	Depth (m)	Hydraulic resistance (C)	Log (C)	Vulnerability AVI
39	Sandy	10.00	30.00	3.00	<1	Extremely high
41	Sandy loam	2.98	30.00	10.07	1 to 2	High
48	Sandy	10.00	30.00	3.00	<1	Extremely high
54	Sandy	10.00	30.00	3.00	<1	Extremely high
59	Sandy loam	2.98	30.00	10.07	1 to 2	High
60	Sandy loam	2.98	30.00	10.07	1 to 2	High
61	Sandy	10.00	30.00	3.00	<1	Extremely high
77	Sandy loam	2.98	30.00	10.07	1 to 2	High
82	Sandy loam	2.98	30.00	10.07	1 to 2	High
85	Sandy	10.00	30.00	3.00	1 to 2	Extremely high
87	Sandy loam	2.98	30.00	10.07	1 to 2	High
89	Sandy loam	2.98	30.00	10.07	1 to 2	High
91	Sandy	10.00	30.00	3.00	<1	Extremely high
93	Sandy loam	2.98	30.00	10.07	1 to 2	High
95	Sandy	10.00	30.00	3.00	<1	Extremely high
97	Sandy loam	2.98	30.00	10.07	1 to 2	High
100	Sandy	10.00	30.00	3.00	<1	Extremely high
103	Sandy	10.00	30.00	3.00	<1	Extremely high
104	Sandy loam	2.98	30.00	10.07	1 to 2	High

Table 4. Aquifer vulnerability index (AVI) for the other main aquifers in Al-Ahsa region

Other main aquifers	K (m/d)	Depth (m)	Hydraulic resistance (C)	Log (C)	Vulnerability AVI class
Dammam	2.76	85	30.74	1–2	High
UmmEr Radhuma	1.38	200	144.68	2–3	Moderate
Aruma	3.37	600	178.06	2–3	Moderate

be increasingly vulnerable to pollution, consistent to the findings of Ahmed et al. (2018), who found that the Hail region (north-western region of SA) is defined by the high and very high vulnerability levels caused by shallow aquifers that possess a lesser depth of vadose zone. Our study, demonstrating the possible risk of groundwater pollution, is a useful resource for policymakers, engineers, environmentalists, and planners for future land use planning.

CONCLUSIONS AND FUTURE RECOMMENDATIONS

In this study, the groundwater analysis showed that the salinity in the Al-Ahsa region, which ranges from 1048 to 1322 mg/L, is a big concern. The TDS, Ca^{2+} , Mg^{2+} , Na^+ and Cl^- of the water were high compared to the US EPA acceptable limits. The dominant water type in aquifers is Na-Cl type, indicating the effects of seawater intrusion on groundwater geochemistry and the study area's geology, which includes rocks with a predominance of CaCO_3 and limestone rock formation as well as sandy, sandy limestone, marl, and shale, as well as subordinate sandstones and siltstones. All Neogene aquifers were classified as highly vulnerable to extremely highly vulnerable class according to the aquifer vulnerability index, which indicates that there is a 47.37% and 52.63% chance of pollution, respectively. The AVI Index method was also performed in the other major aquifers demonstrating that Dammam aquifer was categorized in the high vulnerability class, Er Radhuma and Aruma categorized as moderately vulnerable to contamination. This study could contribute to the improvement of groundwater quality monitoring and be used as a reference for the assessment of water quality in arid and semi-arid climates and the worldwide evolution of water chemistry. Evaluations of aquifer vulnerability assist in pinpointing areas or hotspots where groundwater resources are especially vulnerable to pollution. For example, because toxins have shorter transit periods via shallower groundwater tables, such locations in other regions are more

vulnerable. Aquifer vulnerability assessment helps in implementing effective management strategies to prevent contamination. Stricter laws or zoning restrictions might be necessary in areas with extremely susceptible aquifers to stop any activity that could endanger the quality of the groundwater. The use of pesticides or fertilizers should be prohibited and organic farming with some governmental incentives should be encouraged. Since many aquifers transcend national borders, cooperation with other countries is essential for the efficient management and preservation of shared resources. To address limitations of geological complexity, future research efforts could consider:

- multi-scale investigations at various temporal and spatial scales, which can aid in more thoroughly capturing the variability and complexity of geological systems. This may entail integrating data across scales and resolving variability at different levels by combining field observations, lab tests, and numerical modeling tools
- Tracer tests using naturally occurring or artificially introduced tracers can help delineate groundwater flow paths, identify preferential flow zones, and quantify mixing processes within aquifer systems
- Systematic data collection and cross-temporal comparison of hydrogeochemical trends can be facilitated by establishing long-term groundwater monitoring networks spanning various geological contexts. By keeping a close eye on important metrics, researchers may monitor changes in groundwater quality, evaluate the success of management strategies, and identify emerging patterns or anomalies that might need more inquiry

Given that the cost of remediating a contaminated aquifer is much higher than protecting the existing water resource, these findings can be used by policymakers and planners to prioritize monitoring during environmental health risk assessment projects. Future research should focus on regular monitoring

of nitrate, fluoride, pesticides and their metabolites, pharmaceuticals, veterinary medicines, personal care products like fragrances, cosmetics, dietary supplements, detergents, antimicrobials, microplastics, and potentially toxic trace metals. We further recommend that fertilizer use and discharge of domestic and other agricultural effluents should be restricted in high and very highly vulnerable areas. Since urbanization is on the rise and is affecting the environment as well as the natural resources, further studies investigating urbanization activities such as the development of industrial areas are also required to protect high-value and scanty fresh groundwater resources.

Acknowledgments

This work has been financially supported by the Deanship of Scientific Research, Vice Presidency for Graduate Studies and Scientific Research, King Faisal University, Saudi Arabia [Project No. GRANTA429].

REFERENCES

1. Abdel-Satar A.M., Al-Khabbas M.H., Alahmad W.R., Yousef W.M., Alsomadi R.H., Iqbal T. 2017. Quality assessment of groundwater and agricultural soil in Hail region, Saudi Arabia. *Egyptian Journal of Aquatic Research*, 43(1), 55–64. <https://doi.org/10.1016/j.ejar.2016.12.004>
2. Acharya S., Sharma S.K., Khandegar V. 2018. Assessment of groundwater quality by water quality indices for irrigation and drinking in South West Delhi, India. *Data in Brief*, 18, 2019–2028. <https://doi.org/10.1016/j.dib.2018.04.120>
3. Ahmad A.Y., Al-Ghouti M.A. 2020. Approaches to achieve sustainable use and management of groundwater resources in Qatar: A review. *Groundwater for Sustainable Development*, 11. <https://doi.org/10.1016/j.gsd.2020.100367>
4. Al-Omran A.M., Aly A.A., Al-Wabel M.I., Al-Shayaa M.S., Sallam A.S., Nadeem M.E. 2017. Geostatistical methods in evaluating spatial variability of groundwater quality in Al-Kharj Region, Saudi Arabia. *Applied Water Science*, 7(7), 4013–4023. <https://doi.org/10.1007/s13201-017-0552-2>
5. Al-Omran A.M., Aly A.A., Al-Wabel M.I., Sallam A.S., Al-Shayaa M.S. 2016. Hydrochemical characterization of groundwater under agricultural land in arid environment: a case study of Al-Kharj, Saudi Arabia. *Arabian Journal of Geosciences*, 9(1), 1–17. <https://doi.org/10.1007/s12517-015-2136-5>
6. Al-Omran A.M., Mousa M.A., AlHarbi M.M., Nadeem M.E.A. 2018. Hydrogeochemical characterization and groundwater quality assessment in Al-Hasa, Saudi Arabia. *Arabian Journal of Geosciences*, 11(4), 79. <https://doi.org/10.1007/s12517-018-3420-y>
7. Al-Zarah A.I. 2007. Hydrogeochemical processes of Alkhobar aquifer in eastern region, Saudi Arabia. *Journal of Applied Sciences*, 7(23), 3669–3677. <https://doi.org/10.3923/jas.2007.3669.3677>
8. Al Tokhais A.S., Rausch R. 2008. The Hydrogeology of Al Hassa Springs. *The 3rd International Conference on Water Resources and Arid Environments*, 1, 16–19.
9. Alghamdi A.G., Aly A.A., Aldhumri S.A., Al-Barakaha F.N. 2020. Hydrochemical and quality assessment of groundwater resources in Al-Madinah City, Western Saudi Arabia. *Sustainability (Switzerland)*, 12(8), 1–14. <https://doi.org/10.3390/SU12083106>
10. Aller L., Bennett T., Lehr J.H., Petty R.J., Hackett G. 1987. DRASTIC : A Standardized Method for Evaluating Ground Water Pollution Potential Using Hydrogeologic Settings. *NWWA/EPA--600/2-87-035 Series*. Ada, Oklahoma, U.S. Environmental Protection Agency, 455.
11. Aly A.A., Al-Omran A.M., Alharby M.M. 2015. The water quality index and hydrochemical characterization of groundwater resources in Hafar Albatin, Saudi Arabia. *Arabian Journal of Geosciences*, 8(6), 4177–4190. <https://doi.org/10.1007/s12517-014-1463-2>
12. APHA. 2005. *Standard Methods for the Examination of Water and Wastewater*. Standard Methods. <https://doi.org/ISBN 9780875532356>
13. Bakiewicz W., Milne D.M., Noori M. 1982. Hydrogeology of the Umm ErRadhuma aquifer, Saudi Arabia, with reference to fossil gradients. *Quarterly Journal of Engineering Geology and Hydrogeology*, 15, 105–126.
14. Carol E.S., Kruse E.E., Laurencena P.C., Rojo A., Deluchi M.H. 2012. Ionic exchange in groundwater hydrochemical evolution. Study case: The drainage basin of El Pescado creek (Buenos Aires province, Argentina). *Environmental Earth Sciences*, 65(2). <https://doi.org/10.1007/s12665-011-1318-z>
15. Chen J., Huang Q., Lin Y., Fang Y., Qian H., Liu R., Ma H. 2019. Hydrogeochemical characteristics and quality assessment of groundwater in an irrigated region, Northwest China. *Water (Switzerland)*, 11(1). <https://doi.org/10.3390/w11010096>
16. Clapp R.B., Hornberger G.M. 1978. Empirical equations for some soil hydraulic properties. *Water Resources Research*, 14(4). <https://doi.org/10.1029/WR014i004p00601>
17. Dawood A.S., Jabbar M.T., Al-Tameemi H.H., Baer E.M. 2022. Application of Water Quality Index and Multivariate Statistical Techniques to Assess and Predict of Groundwater Quality with Aid of Geographic Information System. *Journal of Ecological Engineering*, 23(6). <https://doi.org/10.12911/22998993/148195>

18. El-Sayed H.M., Elgendy A.R. 2024. Geospatial and geophysical insights for groundwater potential zones mapping and aquifer evaluation at Wadi Abu Marzouk in El-Nagila, Egypt. *Egyptian Journal of Aquatic Research*. <https://doi.org/10.1016/j.ejar.2023.12.008>
19. El-Sayed H.M., Ibrahim M.I.A., Abou Shagar A.S., Elgendy A.R. 2023. Geophysical and hydrochemical analysis of saltwater intrusion in El-Omayed, Egypt: Implications for sustainable groundwater management. *Egyptian Journal of Aquatic Research*, 49(4). <https://doi.org/10.1016/j.ejar.2023.11.005>
20. Ettazarini S. 2005. Processes of water-rock interaction in the Turonian aquifer of Oum Er-Rabia Basin, Morocco. *Environmental Geology*, 49(2). <https://doi.org/10.1007/s00254-005-0088-x>
21. Fonseca L.M., Domingues J.P., Dima A.M. 2020. Mapping the sustainable development goals relationships. *Sustainability (Switzerland)*, 12(8). <https://doi.org/10.3390/SU12083359>
22. Gogu R.C., Dassargues A. 2000. Current trends and future challenges in groundwater vulnerability assessment using overlay and index methods. *Environmental Geology*, 39(6), 549–559. <https://doi.org/10.1007/s002540050466>
23. Iqbal J., Nazzal Y., Howari F., Xavier C., Yousef A. 2018. Hydrochemical processes determining the groundwater quality for irrigation use in an arid environment: The case of Liwa Aquifer, Abu Dhabi, United Arab Emirates. *Groundwater for Sustainable Development*, 7, 212–219. <https://doi.org/10.1016/j.gsd.2018.06.004>
24. Kumar P., Bansod B.K.S., Debnath S.K., Thakur P.K., Ghanshyam C. 2015. Index-based groundwater vulnerability mapping models using hydrogeological settings: A critical evaluation. In *Environmental Impact Assessment Review*, 51, 38–49. <https://doi.org/10.1016/j.eiar.2015.02.001>
25. Masetti M., Sterlacchini S., Ballabio C., Sorichetta A., Poli S. 2009. Influence of threshold value in the use of statistical methods for groundwater vulnerability assessment. *Science of the Total Environment*, 407(12), 3836–3846. <https://doi.org/10.1016/j.scitotenv.2009.01.055>
26. Mukhopadhyay A., Al-Sulaimi J., Al-Awadi E., Al-Ruwaih F. 1996. An overview of the Tertiary geology and hydrogeology of the northern part of the Arabian Gulf region with special reference to Kuwait. *Earth-Science Reviews*, 40(3–4), 259–295. [https://doi.org/10.1016/0012-8252\(95\)00068-2](https://doi.org/10.1016/0012-8252(95)00068-2)
27. Nasr M., Zahran H.F. 2014. Using of pH as a tool to predict salinity of groundwater for irrigation purpose using artificial neural network. *Egyptian Journal of Aquatic Research*, 40(2). <https://doi.org/10.1016/j.ejar.2014.06.005>
28. Pebesma E.J. 2004. Multivariable geostatistics in S: The gstat package. *Computers and Geosciences*, 30(7), 683–691. <https://doi.org/10.1016/j.cageo.2004.03.012>
29. Phan C.N., Strużyński A., Kowalik T. 2023. Correlation between hydrochemical component of surface water and groundwater in Nida Valley, Poland. *Journal of Ecological Engineering*, 24(12). <https://doi.org/10.12911/22998993/172424>
30. Piper A.M. 1944. A graphic procedure in the geochemical interpretation of water-analyses. *Eos, Transactions American Geophysical Union*, 25(6), 914–928. <https://doi.org/10.1029/TR025i006p00914>
31. Raju N.J., Ram P., Gossel W. 2014. Evaluation of groundwater vulnerability in the lower Varuna catchment area, Uttar Pradesh, India using AVI concept. *Journal of the Geological Society of India*, 83(3), 273–278. <https://doi.org/10.1007/s12594-014-0039-9>
32. Rice E., Baird R., Eaton A., Clesceri L. 2012. *Standard Methods for the Examination of Water and Wastewater*. Standard Methods.
33. Saleh A., Gad A., Ahmed A., Arman H., Farhat H.I. 2023. Groundwater Hydrochemical Characteristics and Water Quality in Egypt's Central Eastern Desert. *Water (Switzerland)*, 15(5). <https://doi.org/10.3390/w15050971>
34. Van Stempvoort D., Ewert L., Wassenaar L. 1993. Aquifer vulnerability index: A GIS - compatible method for groundwater vulnerability mapping. *Canadian Water Resources Journal*, 18(1), 25–37. <https://doi.org/10.4296/cwrj1801025>
35. WHO. 2008. *Guidelines for Drinking-water Quality*. World Health Organization, 1.
36. WHO. 2017. *Guidelines for drinking-water quality: fourth edition incorporating the first addendum*. Geneva. World Health Organization, 4(Licence: CC BY-NC-SA 3.0 IGO.).
37. Wösten J.H.M., Pachepsky Y.A., Rawls W.J. 2001. Pedotransfer functions: Bridging the gap between available basic soil data and missing soil hydraulic characteristics. *Journal of Hydrology*, 251(3–4), 123–150. [https://doi.org/10.1016/S0022-1694\(01\)00464-4](https://doi.org/10.1016/S0022-1694(01)00464-4)
38. Yang J., Liu H., Tang Z., Peeters L., Ye M. 2022. Visualization of Aqueous Geochemical Data Using Python and WQChartPy. *Groundwater*, 60(4). <https://doi.org/10.1111/gwat.13185>
39. Yu C., Yao Y., Hayes G., Zhang B., Zheng C. 2010. Quantitative assessment of groundwater vulnerability using index system and transport simulation, Huangshuihe catchment, China. *Science of the Total Environment*, 408(24), 6108–6116. <https://doi.org/10.1016/j.scitotenv.2010.09.002>